Available online at www.sciencedirect.com
SCIENCE DIRECT®
International Journal of Thermal Sciences 43 (2004) 531–539
International Journal of Thermal Sciences
www.elsevier.com/locate/ijts

Laminar mixed convection of humid air in a vertical channel with evaporation or condensation at the wall

Zouhair Ait Hammou [a], Brahim Benhamou [a], Nicolas Galanis [b,*], Jamel Orfi [c]

[a] *LMFE, département de physique, faculté des sciences Semlalia, Marrakech, Morocco*
[b] *THERMAUS, département de génie mécanique, Université de Sherbrooke, Sherbrooke, Québec, Canada*
[c] *LESTE, École nationale d'ingénieurs de Monastir, Monastir, Tunisia*

Received 10 March 2003; accepted 21 October 2003

Available online 7 January 2004

Abstract

The effects of simultaneous heat and mass transfer on downward laminar flow of humid air in a vertical channel with isothermal wet walls have been studied numerically using an elliptical formulation. The entering air is always warmer than the channel walls but its absolute humidity can be higher or lower than the one corresponding to the wall temperature. Thus, cooling of the air stream is accompanied by either condensation or evaporation. The axial evolutions of the interfacial transverse velocity, of the average air temperature and average vapour mass fraction, of the sensible and latent Nusselt numbers, of the friction factor as well as that of the Sherwood number are presented and analysed for different inlet air conditions. The effects of the buoyancy forces on the hydrodynamic field are very important while their influence on the average air temperature and average mass fraction is small. Even though sensible heat is always transferred from the air to the walls, the latter must be heated when evaporation is important. If evaporation is weak, or if condensation occurs, the walls must be cooled.

Keywords: Double diffusion; Heat and mass transfer; Air cooling; Numerical study; Channel flow

1. Introduction

Confined flows with simultaneous thermal and chemical species diffusion occur in many industrial processes such as the cooling of electronic systems, the chemical deposition of solid layers, the distillation of sea water and in cooling towers. They are therefore studied extensively, mostly numerically since the number of independent variables influencing the hydrodynamic, thermal and concentration fields is quite large and their control in experimental installations is rather difficult.

More specifically, laminar mixed convection in ducts with simultaneous heat and mass transfer between a flowing gas and a liquid wetting the walls has been the subject of a considerable number of publications. Thus, Yan [1] studied the effect of the liquid film thickness and concluded that it can be neglected when the liquid mass flow rate is small. Lee et al. [2] studied ascending flow of cold dry air in a vertical rectangular duct with one wet isothermal wall and three adiabatic dry walls. They showed that, in this case, the aiding buoyancy forces due to temperature and concentration gradients increase the rate of heat and mass transfer over the corresponding values for forced convection. Ali Cherif and Daif [3] considered downward flow of air and a binary liquid film of finite thickness and showed that it is possible to evaporate more water from an ethylene glycol–water liquid mixture than from pure water. Orfi and Galanis [4] analysed the effect of the thermal and solutal Grashof numbers on mixed convection airflow in tubes with uniform concentration and uniform heat flux at the solid-fluid interface. For horizontal tubes, and for vertical tubes with upward flow, they found that the Nusselt and Sherwood numbers as well as the wall shear stress are higher than for forced convection. On the other hand, for a vertical tube with descending flow these three parameters are lower when buoyancy forces are taken into consideration. Lately, Benachour et al. [5] treated downward airflow in a vertical

* Corresponding author.
E-mail addresses: bbenhamou@ucam.ac.ma (B. Benhamou), nicolas.galanis@usherbrooke.ca (N. Galanis), jamel.orfi@fsm.rnu.tn (J. Orfi).

1290-0729/$ – see front matter
doi:10.1016/j.ijthermalsci.2003.10.010

Nomenclature

C	non-dimensional mass fraction, $=(w-w_0)/(w_w-w_0)$	U, V	non-dimensional velocity components
D	mass diffusion coefficient ..... $m{\cdot}s^{-2}$	w	mass fraction (kg of vapour)·(kg of mixture)$^{-1}$
D_h	hydraulic diameter..... m	x	axial coordinate ..... m
f	friction factor	X, Y	non-dimensional coordinates
g	gravitational acceleration..... $m{\cdot}s^{-2}$	*Greek symbols*	
Gr_M	solutal Grashof number, $=g\beta^* D_h^3(w_w-w_0)/\nu^2$	β	coefficient of thermal expansion ..... K^{-1}
Gr_T	thermal Grashof number, $=g\beta D_h^3(T_w-T_0)/\nu^2$	β^*	coefficient of mass fraction expansion
h	half distance between plates ..... m	γ	aspect ratio, $=2h/L$
h_{fg}	enthalpy of evaporation..... $J{\cdot}kg^{-1}$	θ	non-dimensional temperature
k	thermal conductivity ..... $W{\cdot}m^{-1}{\cdot}K^{-1}$	ν	kinematic viscosity ..... $m^2{\cdot}s^{-1}$
L	channel length ..... m	ρ	density..... $kg{\cdot}m^{-3}$
N	Grashof number ratio, $=Gr_M/Gr_T$	ϕ	relative humidity
P	non-dimensional pressure, $=(p-\rho_0 gx)/\rho_0 U_0^2$	Φ	general variable
Pr	Prandtl number	*Subscripts*	
q	heat flux..... $W{\cdot}m^{-2}$	m	mean value
Re	Reynolds number, $=U_0 D_h/\nu$	0	inlet conditions
Sc	Schmidt number, $=\nu/D$	w	wall
T	temperature..... K		

tube with finite liquid film thickness. They showed that the thickness and composition of the liquid film play an important role in determining heat and mass transfer rates. They also presented experimental estimations of the Nusselt number for this configuration.

All these studies of mixed convection with double diffusion considered situations where both heat and mass were added to the air stream. Furthermore, these numerical studies neglected axial diffusion of heat, momentum and chemical species. This approach simplifies the numerical solution of the partial differential equations modeling the flow field as well as the temperature and concentration distributions. On the other hand, this axially parabolic model cannot predict flow reversal that may occur when the flow rate is low and/or when the buoyancy forces are important. The present study differs from previous ones in two important aspects. Firstly, the adopted model includes the axial diffusion terms and, therefore, the equations are elliptical in all directions. Secondly, the conditions under investigation correspond to those encountered in natural air conditioning systems where hot air is in direct contact with cold water and, therefore, heat is removed from the air stream. Such systems are technologically simple and are particularly interesting for regions with a hot dry climate.

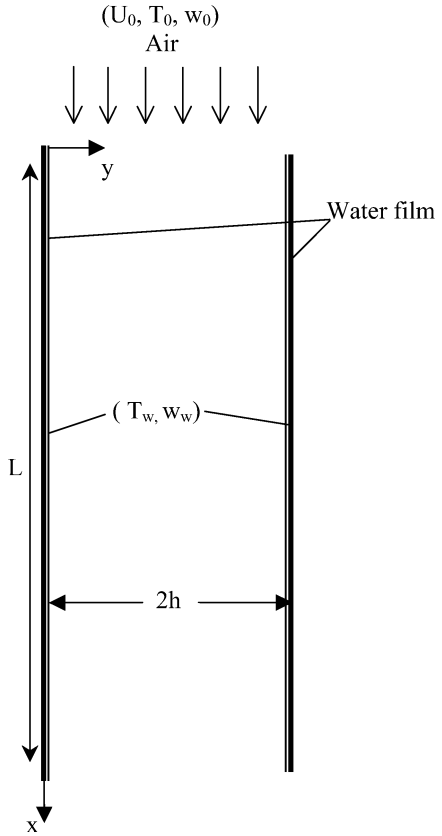

Fig. 1. Schematic representation of system under study.

2. Problem formulation

Atmospheric air with a uniform dry bulb temperature T_0 and a uniform relative humidity ϕ_0 enters a vertical channel with a uniform downward velocity U_0. The channel is formed by two isothermal plates of length L; its width is $2h$ (Fig. 1). The plates are covered by a very thin film of liquid water at T_w. Steady state conditions are considered and the flow is assumed to be laminar. Viscous dissipation as well as the Dufour and Soret effects are assumed to be

negligible as in all the studies cited in the introduction. Finally, the physical properties are assumed to be constant except for the density in the body forces which is considered to be a linear function of temperature and mass fraction:

$$\rho = \rho_0\big[1 - \beta(T - T_0) - \beta^*(w - w_0)\big] \tag{1}$$

It should be noted that for the air–water combination under consideration both β and β^* are positive. However this is not the case for all gas–liquid combinations.

The following reference quantities are used for non-dimensionalisation: the plate length L for linear dimensions, U_0 for the velocity components, $T_w - T_0$ for the temperature difference $T - T_0$ and $w_w - w_0$ for the mass fraction difference $w - w_0$. With this formulation and the above assumptions, the differential equations modeling the problem are:

(a) conservation of mass

$$\frac{\partial U}{\partial X} + \frac{\partial V}{\partial Y} = 0 \tag{2}$$

(b) streamwise momentum equation

$$\left(U\frac{\partial U}{\partial X} + V\frac{\partial U}{\partial Y}\right) = -\frac{\partial P}{\partial X} + \frac{2\gamma}{Re}\left(\frac{\partial^2 U}{\partial X^2} + \frac{\partial^2 U}{\partial Y^2}\right) - \frac{1}{2\gamma Re^2}(Gr_T\theta + Gr_M C) \tag{3}$$

(c) spanwise momentum equation

$$\left(U\frac{\partial V}{\partial X} + V\frac{\partial V}{\partial Y}\right) = -\frac{\partial P}{\partial Y} + \frac{2\gamma}{Re}\left(\frac{\partial^2 V}{\partial X^2} + \frac{\partial^2 V}{\partial Y^2}\right) \tag{4}$$

(d) conservation of energy

$$\left(U\frac{\partial \theta}{\partial X} + V\frac{\partial \theta}{\partial Y}\right) = \frac{2\gamma}{Pr\,Re}\left(\frac{\partial^2 \theta}{\partial X^2} + \frac{\partial^2 \theta}{\partial Y^2}\right) \tag{5}$$

(e) species conservation

$$\left(U\frac{\partial C}{\partial X} + V\frac{\partial C}{\partial Y}\right) = \frac{2\gamma}{Sc\,Re}\left(\frac{\partial^2 C}{\partial X^2} + \frac{\partial^2 C}{\partial Y^2}\right) \tag{6}$$

Eq. (3) indicates that for such double diffusion problems two different Richardson numbers must be considered: the thermal Richardson number $Ri_T = Gr_T/Re^2$ and the solutal Richardson number $Ri_M = Gr_M/Re^2$. Alternatively, some authors [6] cast the problem in terms of the thermal Grashof or Richardson number and the ratio $N = Ri_M/Ri_T = Gr_M/Gr_T$. Here we shall use the two Grashof numbers to define the flow conditions since either one could be equal to zero. Positive values of Gr_T and Gr_M indicate that the thermal and solutal buoyancy forces act upwards. These conditions prevail when $T_w > T_0$ and $w_w > w_0$ since β and β^* are positive for the air–water combination under consideration.

It should be noted that this system of coupled non-linear partial differential equations is elliptical in both the X and Y directions contrary to all the previous studies cited in the introduction, which adopted an axially parabolic formulation. That approach simplifies the formulation (boundary conditions at the outlet are not required) and the corresponding PDEs can be solved with a marching technique, which requires relatively little computer memory. On the other hand, the axially parabolic models are less accurate when the buoyancy forces are important and cannot predict flow reversal, which is most likely to occur when both buoyancy forces act opposite to the flow direction. As far as we can ascertain, the present study is the first using the full elliptical equations to model simultaneous heat and mass transfer.

The boundary conditions for the problem under consideration are:

at the inlet ($X = 0, 0 < Y < \gamma$):

$$U = 1 \text{ and } V = \theta = 0 \tag{7}$$

at the outlet ($X = 1, 0 < Y < \gamma$):

all axial derivatives are zero (8)

at the walls ($Y = 0$ and $Y = \gamma, 0 < X < 1$):

$$U = 0,\ V = V_e,\ C = \theta = 1 \tag{9}$$

where the non-dimensional transverse velocity at the interface is [2]

$$V_e = (-2\gamma/Re\,Sc)(w_w - w_0)(1 - w_w)^{-1}(\partial C/\partial Y)_{Y=0} \tag{10}$$

and the mass fraction at the wall w_w corresponds to the saturation conditions at T_w.

Heat transfer between the wet wall and the humid air is the sum of a sensible and a latent component [2]:

$$q_t = q_s + q_l = k(\partial T/\partial y)_{y=0} + \rho D h_{fg}(1 - w_w)^{-1}(\partial w/\partial y)_{y=0} \tag{11}$$

Therefore, the Nusselt number

$$Nu_t = hD_h/k = q_t D_h/k(T_w - T_m) = Nu_s - Nu_l \tag{12}$$

where

$$Nu_s = -2\gamma(1 - \theta_m)^{-1}(\partial\theta/\partial Y)_{Y=0} \tag{13a}$$

$$Nu_l = 2\gamma S(1 - \theta_m)^{-1}(\partial C/\partial Y)_{Y=0} \tag{13b}$$

and

$$S = (\rho D h_{fg}/k)(w_w - w_0)(1 - w_w)^{-1}(T_w - T_0)^{-1} \tag{13c}$$

Mass transfer at the interface is characterized by the Sherwood number

$$Sh = h_M D_h/D = -2\gamma(1 - w_m)^{-1}(\partial C/\partial Y)_{Y=0} \tag{14}$$

while the friction coefficient is

$$f\,Re = 4\gamma(\partial U/\partial Y)_{Y=0} \tag{15}$$

Table 1
Effects of discretisation on calculated results

No. of nodes	$x/L = 0.021$	$x/L = 0.1$	$x/L = 0.36$	$x/L = 0.98$
		Values of Nu_s		
100×35	10.4926	8.20026	7.69659	7.559
200×70	10.3954	8.20105	7.7521	7.554
		Values of $f\,Re$		
100×35	46.0972	37.9653	27.9048	23.957
200×70	45.8838	38.1714	27.9435	24.020

3. Numerical solution

The thermophysical properties are evaluated at a temperature and concentration given by the 1/3 law from the expressions given by Lin et al. [7]. All the results presented here have been calculated with $L/2h = 65$ ($\gamma = 0.01538$).

The solution of the PDEs modeling the flow field is based on the method of control volumes proposed by Patankar [8]. Velocity components are calculated at the interfaces of these control volumes while the transportable quantities Φ are evaluated at their centres. The velocity-pressure coupling is treated with the SIMPLER algorithm [8]. Convergence of this iterative procedure is declared when

$$\mathrm{Max}\left(\left(\Phi_{i,j}^{n+1} - \Phi_{i,j}^{n}\right)/\Phi_{i,j}^{n+1}\right) < 10^{-5} \tag{16}$$

The discretisation grid is non-uniform in both the streamwise and transverse directions with greater node density near the inlet and the walls where the gradients are expected to be more significant. The effect of the number of nodes on the calculated results is shown for typical conditions in Table 1. Since the increase of the number of nodes by a factor of four (from 100×35 to 200×70) results in changes of less than 1% on the values of the Nusselt number and of the friction coefficient, the 100×35 discretisation was deemed to be sufficiently accurate. All the results presented in this text have therefore been calculated using 100 and 35 nodes in the X and Y directions, respectively.

Validation of the model and the computer code has been carried out in several steps. First, the calculated axial evolution of the Nusselt number for hydrodynamically and thermally developing forced convection was very close with corresponding published results [9] except in the immediate vicinity of the channel inlet. The influence of axial diffusion, which was not included in the previous study, explains the observed difference in that region. Second, the calculated sensible and latent Nusselt numbers for mixed convection with heat and mass transfer have been compared with corresponding results by Yan and Lin [10]. As seen in Fig. 2 the agreement between these two sets of results is satisfactory. The small differences are due to the imprecision associated with the digitalisation of their graphical results and to the effect of axial diffusion, which was not taken into account by Yan and Lin [10]. In view of these successful comparisons, we conclude that the model and the computer code are reliable and can be used to analyse the problem under consideration.

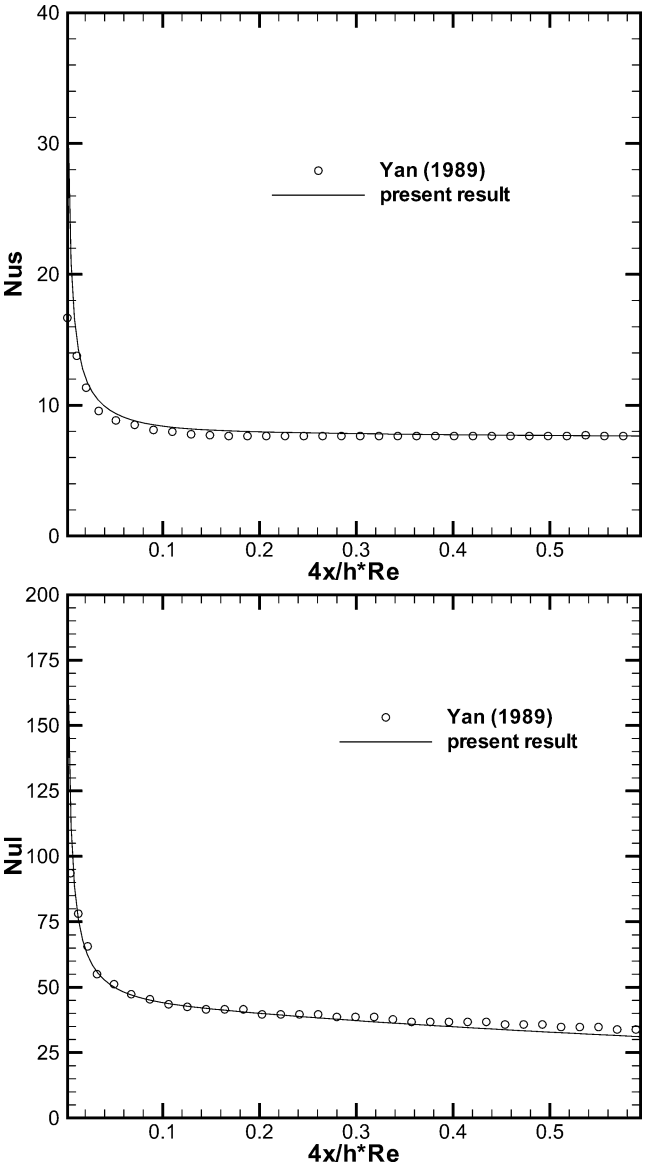

Fig. 2. Validation of calculated Nusselt numbers ($T_w = 40\,^\circ$C, $T_0 = 20\,^\circ$C, $\phi_0 = 50\%$, $Re = 400$).

4. Results and discussion

As noted by Lee et al. [2] the two Grashof numbers in Eq. (3) are not independent since w_w is related to T_w. Since we are interested in studying the effect of the inlet conditions on the flow field, we have fixed the following conditions:

$$Pr = 0.7, \qquad Sc = 0.58, \qquad Re = 300, \qquad T_w = 20\,^\circ\mathrm{C}$$
$$\text{(hence } w_w = 14.5 \text{ (g vap)}\cdot\text{(kg moist air)}^{-1} \tag{17}$$

The chosen combinations of T_0 and ϕ_0 as well as the corresponding values of the two Grashof numbers and other relevant parameters are specified in Table 2. Negative

Table 2
Values of parameters for cases under study

Case #	T_0 [°C]	ϕ_0 [%]	w_0 [g·kg^{-1}]	Gr_T	Gr_M	$\lvert N\rvert$
1	40	10	4.56	−74576	7142	0.0958
2	40	30	13.90	−74717	559	0.0075
3	40	50	23.52	−74860	−6123	0.0818
4	45	10	5.94	−89975	6042	0.0672
5	30	10	2.62	−40077	8876	0.2215

Grashof numbers indicate that the corresponding buoyancy force acts in the direction of gravity and aids the entering flow. The absolute value of the Grashof ratio N is quite small indicating that, for the cases under consideration, the hydrodynamic field is influenced more by thermal buoyancy, which acts in the flow direction (see Eq. (3)). The five cases considered here are quite different from those in other similar studies. For example, in [1] both buoyancy forces oppose the flow, the values of N are higher but the thermal Grashof numbers are considerably smaller than in Table 2; in [2] the values of N and Gr_T are higher than in Table 2 and both buoyancy forces act in the flow direction but the geometry is different; in [4] cases with both buoyancy forces aiding or opposing the flow have been considered with $N = 0, 1, \infty$ but the geometry and thermal boundary condition are different from those in the present study; and, finally, in [7] both buoyancy forces aid the flow, the values of N are higher but the values of Gr_T are considerably lower than in Table 2. Furthermore, it should be noted that in these four studies [1,2,4,7] the conditions were such that mass transfer always occurred by evaporation of the liquid film whereas in the present one conditions that lead to evaporation and condensation have been included. For each of the five combinations of T_0 and ϕ_0 in Table 2 the system of PDEs has been solved twice: once with the values of Gr_M, Gr_T specified in Table 2 and a second time with $Gr_M = Gr_T = 0$ (i.e., for forced convection). By comparing these results it is possible to identify the effects of the buoyancy forces on the flow field.

Fig. 3(a) and (b) show the effect of T_0 and ϕ_0, respectively, on the axial evolution of the non-dimensional transverse velocity at the interface. Positive values of V_e indicate flow towards the plane of symmetry of the channel. It follows that in cases 1, 4 and 5 water from the film is evaporated and transferred to the airflow while in case 3 vapour is removed from the airflow, condensed and transferred to the film. In case 2 the value of V_e is essentially zero indicating that phase change and interfacial mass transfer are negligible for this combination of variables. These results are consistent with the relative values of w_0 and w_w: when $w_w > w_0$ (as in cases 1, 4 and 5) vapour flows from the film to the air stream while when $w_w < w_0$ (as in case 3) it flows in the opposite direction and when $w_w \approx w_0$ there is essentially no vapour flow. It should be noted that, at a given axial position, V_e decreases as T_0 and ϕ_0 increase and that it tends uniformly to zero as x/L increases. This asymptotic behaviour is obviously due to the fact that the temperature

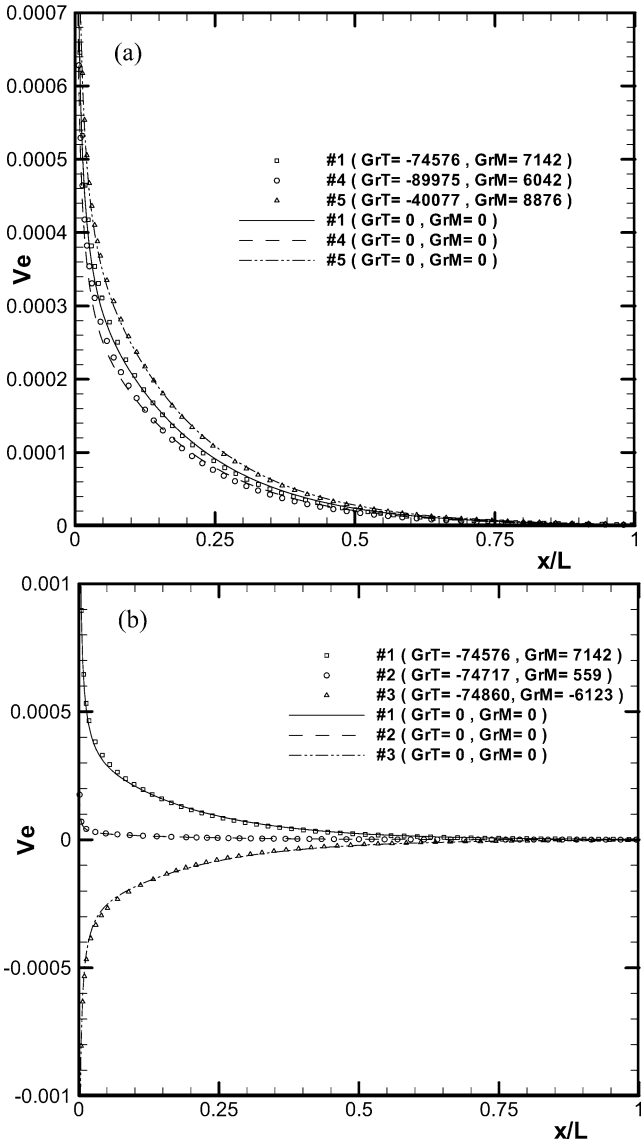

Fig. 3. Axial evolution of the non-dimensional vapour velocity at the interface.

and absolute humidity of the air approach the corresponding wall values as x/L increases. Finally, comparison of the results for mixed and forced convection show that the effect of the buoyancy forces is quite small except in the case of the highest inlet temperature for which differences of up to 10% are observed in the developing region. In general, near the channel inlet, absolute values of V_e for mixed convection are slightly bigger than those for forced convection while the opposite is true in the downstream region.

Fig. 4(a) and (b) show the resulting effects on the axial evolution of the average vapour mass fraction. In cases 1, 4 and 5 w_m increases with x while in case 3 it decreases. In case 2, w_m stays essentially constant. In all cases its value at the channel outlet tends towards the imposed wall condition. This result is consistent with the fact that the corresponding value of V_e tends to zero. When w_m increases (evaporation at the wall) the values for mixed convection are slightly

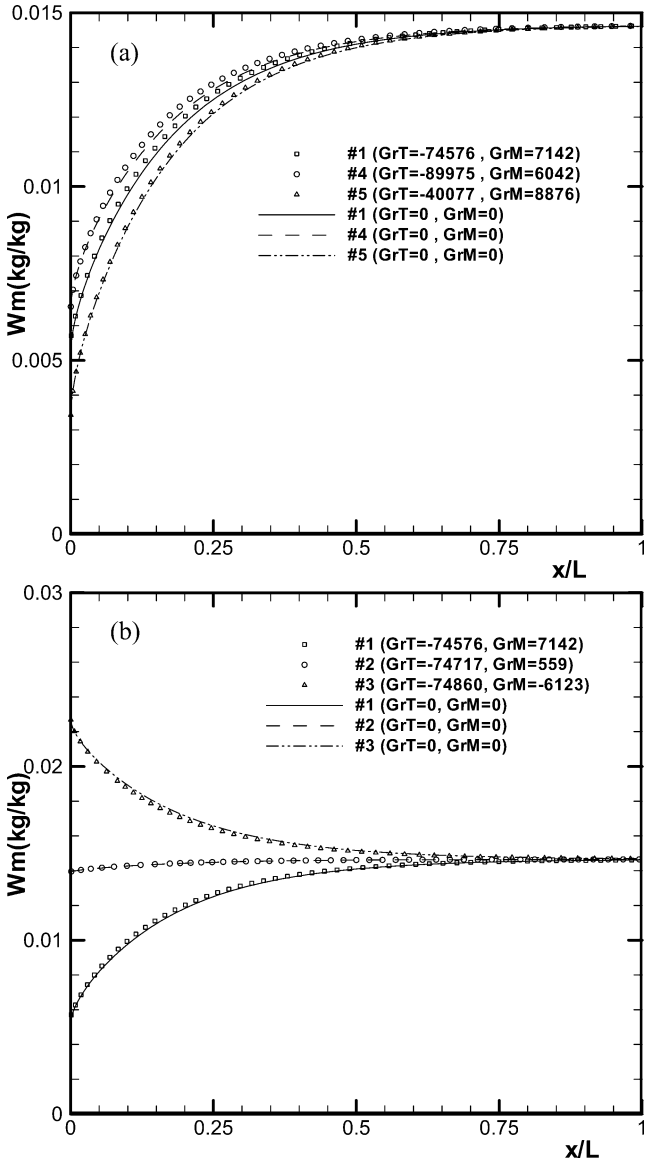

Fig. 4. Axial evolution of the average mass fraction.

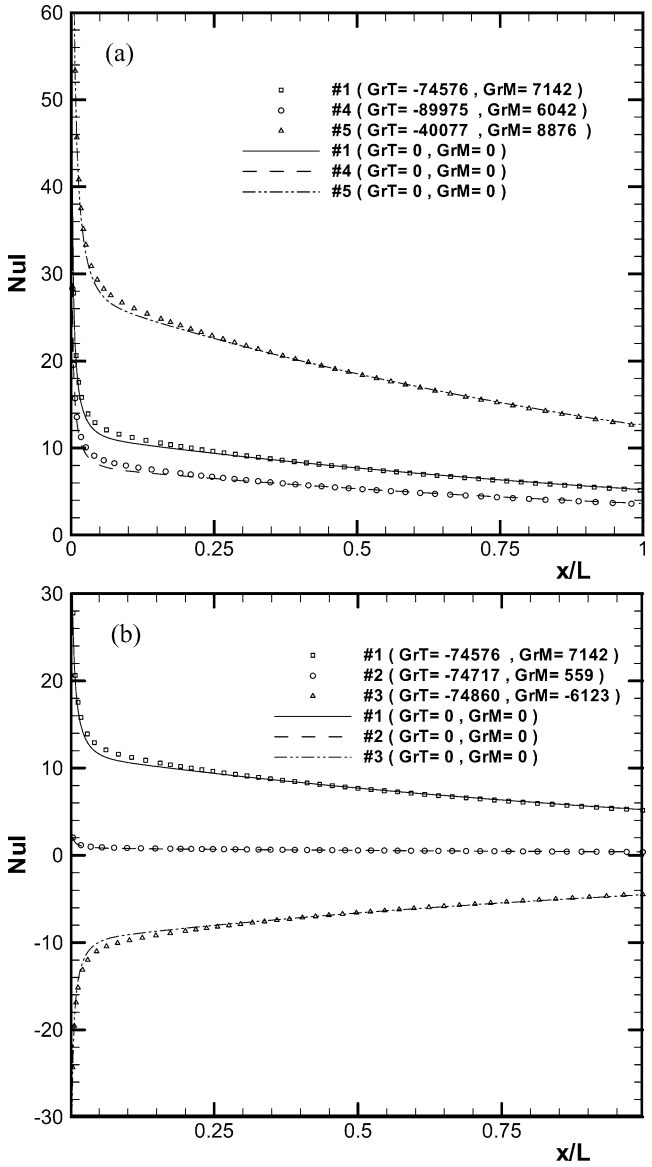

Fig. 5. Axial evolution of the latent Nusselt number.

bigger than those for forced convection. On the other hand, when w_m decreases (condensation at the wall) the opposite is true. In either case, these results indicate that changes in the average mass fraction occur slightly earlier when buoyancy forces are taken into consideration. The results of Fig. 4 also indicate that, at a fixed axial position, w_m increases as T_0 increases and/or as ϕ_0 increases.

Fig. 5 shows the corresponding axial evolution of the latent Nusselt number. According to Eqs. (13b) and (13c) positive values of Nu_l correspond to evaporation of the film (cases 1, 4 and 5) while negative values indicate that condensation takes place (case 3). In case 2 for which there is practically no mass transfer, the values of Nu_l are essentially zero. These results show that, at a given axial position, Nu_l decreases as both T_0 and ϕ_0 increase. Yan [10] attributes these effects to the value of the parameter S (Eq. (13c)) which increases when T_0 and ϕ_0 increase. Once again the effect of buoyancy forces is restricted to the developing region and is rather small. The absolute value of Nu_l for mixed convection is never smaller than the corresponding value for forced convection. The axial evolution of Nu_l for the cases with evaporation (cases 1, 4 and 5) is qualitatively similar to that shown in [2].

Fig. 6(a) and (b), respectively, show the effect of T_0 and ϕ_0 on the axial evolution of the average air temperature. We notice that the air is being cooled in all cases, whether with evaporation (cases 1, 4 and 5), with condensation (case 3) or without mass transfer (case 2). In all cases T_m tends towards the imposed wall temperature. The effect of the inlet humidity is negligible while that of buoyancy forces increases as the inlet temperature increases but remains fairly small even for the highest value of T_0 considered here. These results indicate the average temperature decreases faster when buoyancy is taken into account.

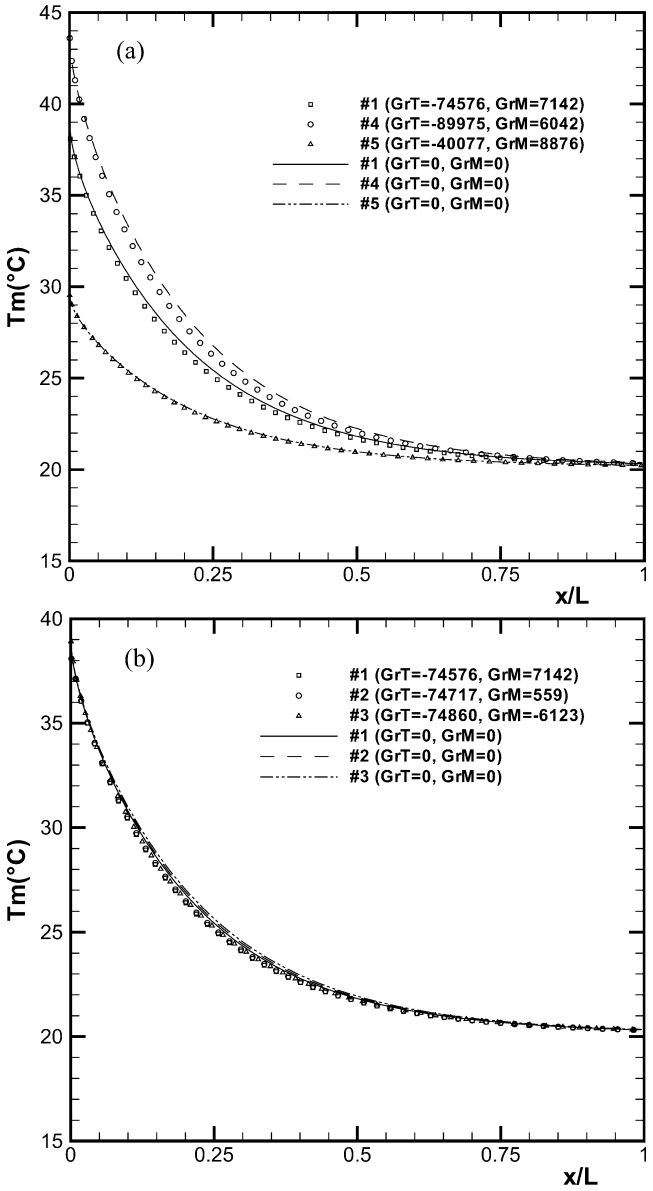

Fig. 6. Axial evolution of the average air temperature.

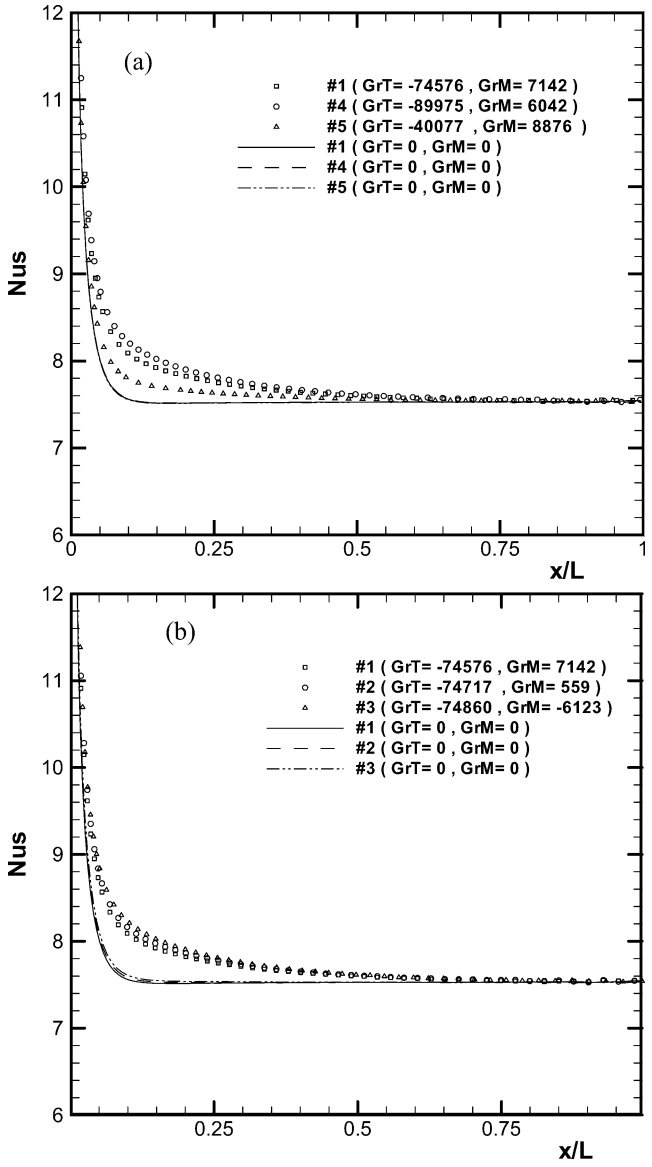

Fig. 7. Axial evolution of the sensible Nusselt number.

Fig. 7(a) and (b) show corresponding results for the sensible Nusselt number. Since the air is always warmer than the liquid film, q_s is always directed towards the walls and, according to Eq. (13a), Nu_s is always positive. In all cases Nu_s decreases monotonically towards the same asymptotic value, $Nu_{s\infty} = 7.54$, which is equal to the analytical value for fully developed forced convection [10]. This result provides additional proof that the adopted model and numerical scheme are valid and precise. This tendency has also been reported by Lin et al. [7], Yan [6] and Orfi and Galanis [4]. Very close to the channel inlet the values of Nu_s are the same for both forced and mixed convection since in this region temperature and concentration gradients are very small. In the developing region however, Nu_s increases as T_0 increases and the values for mixed convection are approximately 10% higher than those for forced convection. The effect of ϕ_0 is very small, although values of Nu_s for flow with condensation (case 3) are slightly higher than those for flow with evaporation (case 1).

It should be noted that in case 2, for which there is practically no mass transfer and Nu_l is close to zero, the value of Nu_t is, according to Eq. (12), essentially equal to that of Nu_s. Since the latter is positive (heat flux from the gas to the walls) over the entire length of the channel, heat must be removed from the walls at all axial positions to maintain their temperature at $T_w = 20\,^{\circ}\mathrm{C}$. In case 3, for which condensation occurs ($Nu_l < 0$), the value of Nu_t is, according to Eq. (12), greater than that of Nu_s over the entire length of the channel. This indicates that the walls must be cooled at all axial positions and the heat which must be removed is everywhere greater than for case 2. On the other hand, in cases 1, 4 and 5 for which evaporation takes place, Nu_l is positive. For the lowest inlet air temperature

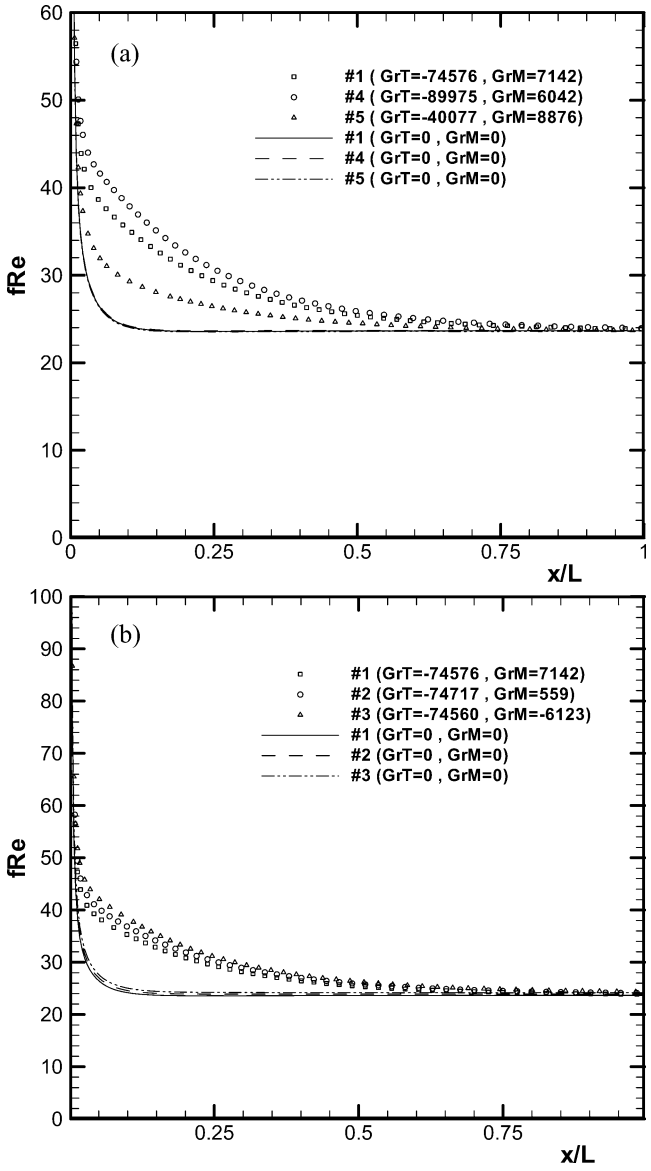

Fig. 8. Axial evolution of the friction coefficient.

(case 5) Nu_l is considerably higher than Nu_s over the entire channel length. Therefore Nu_t and q_t are negative everywhere, indicating that heat must be supplied externally to the walls to maintain them at $T_w = 20\,^{\circ}\mathrm{C}$. For the highest inlet temperature (case 4) Nu_l is again positive but is smaller than Nu_s over the entire channel length. Therefore Nu_t and q_t are positive, i.e., heat must be removed from the walls at all axial positions. The situation is quite different in case 1: for this combination of variables, Nu_l is higher than Nu_s near the channel inlet but the opposite is true near its outlet. Therefore, in this case, heat must be supplied to the walls near the inlet and removed from them near the outlet.

The axial evolution of the friction factor is shown in Fig. 8. This parameter decreases monotonically as the fluid moves downstream towards the same asymptotic value, $f\,Re_\infty = 24$, which is equal to the analytical value for fully developed forced convection [9]. This tendency has also

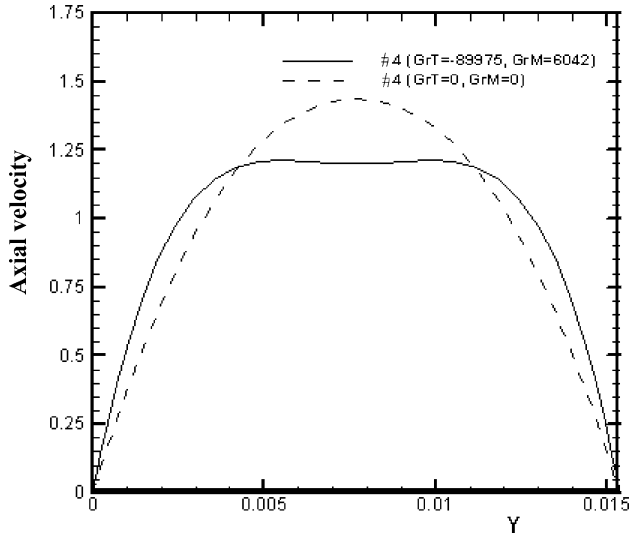

Fig. 9. Velocity profiles at $X = 0.2$.

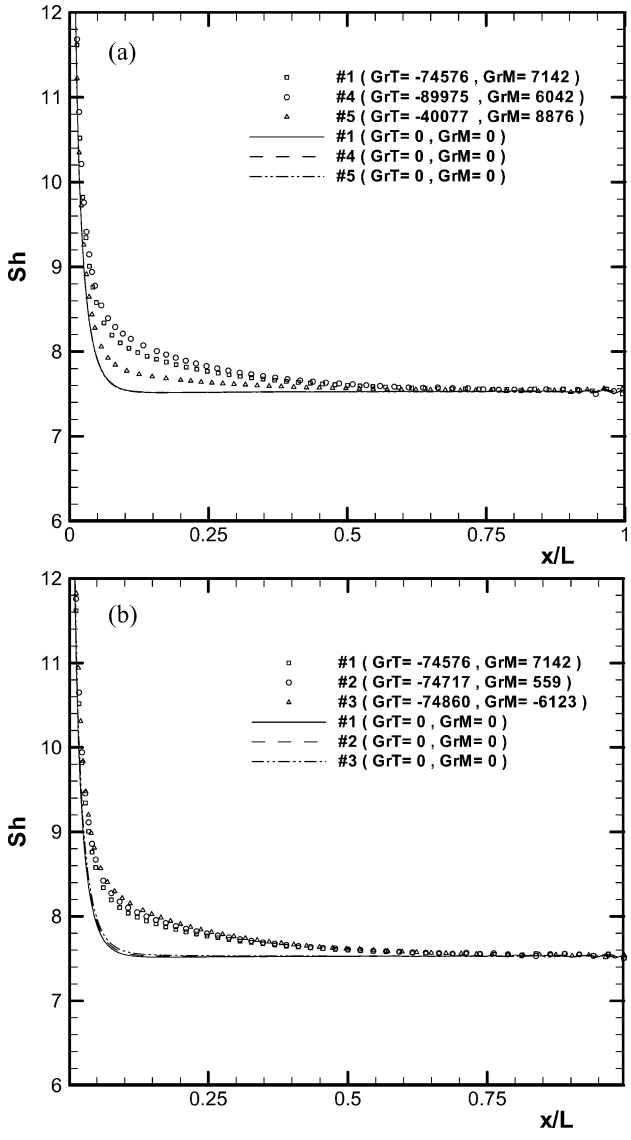

Fig. 10. Axial evolution of the Sherwood number.

been reported by Yan [6] and Orfi and Galanis [4]. Very close to the channel inlet the values of $f\,Re$ are the same for both forced and mixed convection for the reason invoked in the previous paragraph. On the other hand, in the developing region the values for mixed convection (which increase with both T_0 and ϕ_0) are considerably higher than those for forced convection. This significant effect is due to the modification of the axial velocity profiles by the buoyancy forces. Fig. 9 illustrates this modification for a particular combination of operating conditions. For forced convection the velocity decreases monotonically as the distance from the mid-plane increases. For mixed convection, the colder fluid in the vicinity of the walls is accelerated in the direction of flow by the downward acting thermal buoyancy force and the maximum velocity does not occur at the channel mid-plane. The velocity gradient at the wall, as well as the resulting wall shear stress and friction factor, are therefore higher in the case of mixed convection as shown in Fig. 8.

Finally, Fig. 10(a) and (b), respectively, show the effect of T_0 and ϕ_0 on the axial evolution of the Sherwood number. According to Eq. (14) this parameter is positive whether evaporation or condensation takes place. In all cases the value of Sh tends towards the same asymptotic value, $Sh_\infty = 7.54$, which is equal to the analytical value for fully developed forced convection. This tendency has also been reported by Lin et al. [7], Yan [6] and Orfi and Galanis [4]. The effect of the buoyancy forces in the developing region is evident. In this region, Sh increases as T_0 increases while the effect of ϕ_0 is small as in the case of Nu_s. In fact, the axial distributions of Sh are very similar to those of Nu_s as a result of the close values of the Prandtl and Schmidt numbers.

5. Conclusion

The effects of simultaneous cooling and mass transfer on the downward laminar flow of humid air in an isothermal vertical channel with wet walls have been studied numerically. Condensation occurs when the vapour mass fraction at the inlet is higher than the corresponding saturation value at the wall temperature. In the opposite case, evaporation takes place. For fixed wall conditions an increase of the inlet air temperature results in a small increase of the sensible Nusselt number and a significant decrease of the latent Nusselt number. The effect of buoyancy forces on the latent Nusselt numbers is small. On the other hand, the axial velocity profiles, the friction factor, the sensible Nusselt number and the Sherwood number are significantly influenced by buoyancy forces. The friction factor and the Sherwood number increase with both inlet air temperature and inlet air humidity.

References

[1] W.M. Yan, Mixed convection heat transfer in a vertical channel with film evaporation, Canad. J. Chem. Engrg. 71 (1993) 54–62.

[2] K.T. Lee, H.L. Tsai, W.M. Yan, Mixed convection heat and mass transfer in vertical rectangular ducts, Internat. J. Heat Mass Transfer 40 (1997) 1621–1631.

[3] A. Ali Cherif, A. Daif, Étude numérique du transfert de chaleur et de masse entre deux plaques planes verticales en présence d'un film de liquide binaire ruisselant sur l'une des plaques chauffées, Internat. J. Heat Mass Transfer 42 (1999) 2399–2418.

[4] J. Orfi, N. Galanis, Developing laminar mixed convection with heat and mass transfer in horizontal and vertical tubes, Internat. J. Thermal Sci. 41 (2002) 319–331.

[5] K. Benachour, L. Pietri, B. Zeghmati, J. Bresson, Étude numérique et expérimentale de l'évaporation en convection mixte d'un film liquide ruisselant dans un cylindre vertical, Trans. Canad. Soc. Mech. Engrg. 26 (2002) 87–108.

[6] W.M. Yan, Transport phenomena of developing laminar mixed convection heat and mass transfer in inclined rectangular ducts, Internat. J. Heat Mass Transfer 38 (1995) 2905–2914.

[7] T.F. Lin, C.J. Chang, W.M. Yan, Analysis of combined buoyancy effects of thermal and mass diffusion on laminar forced convection heat transfer in a vertical tube, ASME J. Heat Transfer 110 (1988) 337–344.

[8] S.V. Patankar, Numerical Heat Transfer and Fluid Flow, Hemisphere/McGraw-Hill, New York, 1980.

[9] R.K. Shah, A.L. London, Laminar Flow Forced Convection in Ducts, Academic Press, New York, 1978.

[10] W.M. Yan, T.F. Lin, Effects of wetted wall on laminar mixed convection in a vertical channel, J. Thermophys. 3 (1989) 94–96.